

Microstructure and ferroelectric properties of epitaxial cation ordered PbSc_{0.5}Ta_{0.5}O₃ thin films grown on electroded and buffered Si(100)

Anuj Chopra, Daniel Pantel, Yunseok Kim, Marin Alexe, and Dietrich Hesse

Citation: *J. Appl. Phys.* **114**, 084107 (2013); doi: 10.1063/1.4819384

View online: <http://dx.doi.org/10.1063/1.4819384>

View Table of Contents: <http://jap.aip.org/resource/1/JAPIAU/v114/i8>

Published by the [AIP Publishing LLC](#).

Additional information on *J. Appl. Phys.*

Journal Homepage: <http://jap.aip.org/>

Journal Information: http://jap.aip.org/about/about_the_journal

Top downloads: http://jap.aip.org/features/most_downloaded

Information for Authors: <http://jap.aip.org/authors>

ADVERTISEMENT



AIP Advances

Now Indexed in
Thomson Reuters
Databases

Explore AIP's open access journal:

- Rapid publication
- Article-level metrics
- Post-publication rating and commenting

Microstructure and ferroelectric properties of epitaxial cation ordered $\text{PbSc}_{0.5}\text{Ta}_{0.5}\text{O}_3$ thin films grown on electroded and buffered Si(100)

Anuj Chopra,^{1,2} Daniel Pantel,¹ Yunseok Kim,^{1,3} Marin Alexe,¹ and Dietrich Hesse¹

¹Max Planck Institute of Microstructure Physics, Weinberg 2, D-06120 Halle (Saale), Germany

²Faculty of Science and Technology, MESA + Institute for Nanotechnology, University of Twente, P.O. Box 217, 7500 AE Enschede, The Netherlands

³School of Advanced Materials Science & Engineering, Sungkyunkwan University (SKKU), Suwon, Gyeonggi-do 440-746, South Korea

(Received 8 July 2013; accepted 11 August 2013; published online 27 August 2013)

Epitaxial $\text{PbSc}_{0.5}\text{Ta}_{0.5}\text{O}_3$ (001) films with an epitaxial LaNiO_3 bottom electrode were deposited on $\text{CeO}_2/\text{yttria-stabilized zirconia}$ -buffered Si (100) substrates. Crystal orientation, in-plane and out-of-plane lattice parameters, surface morphology, and microstructure were analyzed by X-ray diffraction, X-ray reciprocal lattice mapping measurements, atomic force microscopy, and transmission electron microscopy, respectively. XRD superstructure reflections indicate that the films are cation ordered. Polarization-field and switching current-voltage hysteresis curves were measured at room temperature. The measured spontaneous polarization P_s , remnant polarization P_r , and coercive voltage V_c were found to be $14 \mu\text{C}/\text{cm}^2$, $4 \mu\text{C}/\text{cm}^2$, and 1.1 V, respectively, at room temperature. Furthermore, field as well as frequency dependence of the dielectric constant were measured at room temperature. Piezoelectric measurements performed on these PST films showed a sharp non-linearity, which is attributed to the possibility of field induced phase transition and/or percolation of polar nano regions. © 2013 AIP Publishing LLC. [<http://dx.doi.org/10.1063/1.4819384>]

I. INTRODUCTION

Ferroelectric thin films have attracted attention owing to the desirable functional properties of many perovskite oxides, such as ferroelectricity, pyroelectricity, and piezoelectricity. They have been used in several applications including ferroelectric random access memories (FeRAMs), pyroelectric detectors, micro-electro-mechanical systems (MEMS), piezoelectric actuators, etc.¹⁻⁷ Ferroelectric thin films have the capacity to integrate economical size design and high performance efficiency. Epitaxial growth of ferroelectric thin films on existing silicon circuitry could thus pave the way to fabricating even thinner, more efficient devices, because of their minimal leakage, optical scattering and other improved properties compared to polycrystalline films.¹

The pyroelectric effect in ferroelectrics has been used long for imaging and detection of infrared radiation (IR), but only a few of them have become subject of intense research for uncooled IR detection and imaging sensors.⁸ Among them $\text{PbSc}_{0.5}\text{Ta}_{0.5}\text{O}_3$ (PST) is very promising because of its high figure of merit in IR detection.⁹ So deposition of high-quality PST thin films on Si substrates is desirable, however, it still involves technical difficulties due to the large lattice mismatch (31%), structural incompatibility, and thermal expansion mismatch¹⁰ (nearly a factor of 3) between both.

PST is well known as a relaxor ferroelectric with Curie temperature between 0 and 26 °C, depending on the degree of cation-ordering on the B sites.¹¹ In this paper, we report the epitaxial growth by pulsed laser deposition (PLD), microstructure and ferroelectric behavior of epitaxial PST (100) films on buffered Si (100) substrates.

II. EXPERIMENTAL PROCEDURE

PLD is a good method to ensure stoichiometric transfer of components from a target to a thin film and to prepare multilayers.¹² The epitaxial growth of oxide thin films on silicon substrates is a challenging process due to oxidation of silicon to amorphous silicon oxide and possible diffusion and/or reaction processes between film and substrate. We achieved this aim by using an epitaxial buffer layer of CeO_2 and yttria-stabilized (10 mol. %) zirconia (YSZ) between the PST film and the silicon substrate. YSZ grows epitaxially on Si (100) and is inert to it.^{13,14} CeO_2 is often used as second buffer layer to promote the epitaxial growth of LaNiO_3 (LNO) as a bottom electrode.¹⁵⁻¹⁸ All the films were deposited *in situ* by ablating stoichiometric targets of YSZ, CeO_2 , LNO, and PST with KrF excimer laser pulses (wavelength of 248 nm, pulse duration 20 ns) with a 5 Hz repetition rate. An epitaxial YSZ thin layer was deposited on natively oxidized Si wafer, with a laser fluence of $2 \text{ J}/\text{cm}^2$. The Si (100) substrate was cleaned with acetone and ethanol before mounting to the substrate heater. The base pressure in the chamber was 5×10^{-7} mbar before raising the substrate temperature. YSZ was deposited at 750 °C for 3 min (900 pulses) in the base pressure and then oxygen pressure was increased to 6.5×10^{-4} mbar. CeO_2 and LNO films were deposited at 750 °C and 650 °C in 5.5×10^{-4} mbar and 0.4 mbar oxygen pressures, respectively, with a laser fluence of $2 \text{ J}/\text{cm}^2$ each. The epitaxial PST films were deposited at 550 °C with a laser fluence of $1.5 \text{ J}/\text{cm}^2$. More experimental details are described elsewhere.¹⁹ For electrical measurements, Pt top electrodes were deposited through a metal shadow mask (electrode size of ca. $40 \times 40 \mu\text{m}^2$) by radio frequency sputtering at room temperature.

Crystallographic characterization was performed by means of a Philips X'Pert MRD X-ray diffractometer with Cu $K\alpha$ radiation. Samples for transmission electron microscopy (TEM) were prepared by using mechanical and ion-beam based standard techniques. TEM and electron diffraction investigations were carried out by a Philips CM20T at 200 kV. Polarization-voltage (P - V) hysteresis loop and switching current-voltage (I - V) characteristics of the PST films were recorded by a ferroelectric tester (TF analyzer 2000, aixACCT)). Dielectric constants were calculated from the capacitance measured by a Hewlett Packard 4194 A impedance analyzer using a small ac signal of 100 mV. Local piezoelectric response and switching polarization were investigated by a commercial atomic force microscope (XE-100, Park Systems) in the piezoresponse force microscopy (PFM) mode.

III. RESULTS AND DISCUSSIONS

An XRD pattern of PST and LNO films on CeO_2/YSZ -buffered Si (100) substrate is shown in Fig. 1(a). The PST film consists of a pure perovskite phase; no pyrochlore phase was observed. Superstructure reflections of type $(\frac{1}{2} \frac{1}{2} \frac{1}{2})$ were observed at $2\theta \approx 18.8^\circ$, recorded at $\psi = 54.7^\circ$, as shown in the inset of Fig. 1(b). The average degree of order is calculated by using the integrated area of the superstructure peak $(\frac{1}{2} \frac{1}{2} \frac{1}{2})$ compared to a reference peak (111) in the material

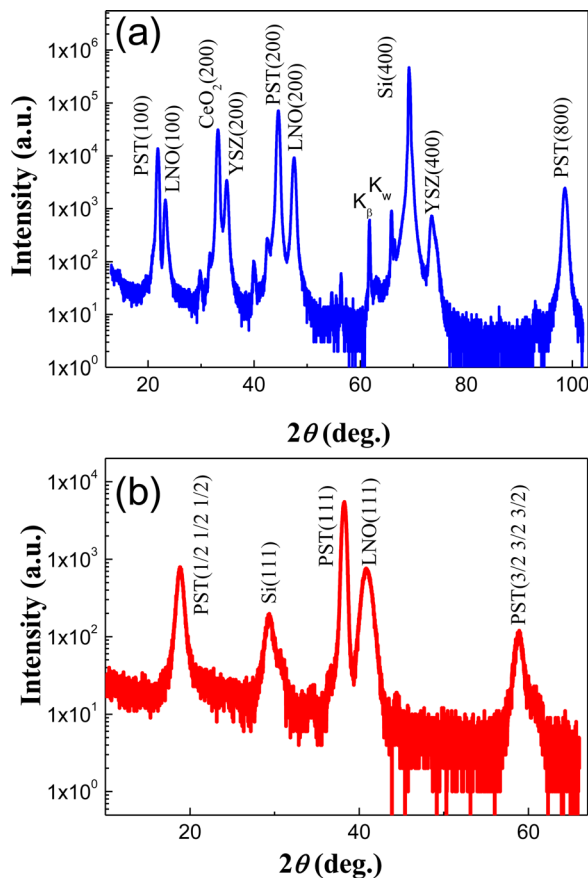


FIG. 1. (a) XRD θ - 2θ scan of the heterostructure PST/LNO/ CeO_2 /YSZ/Si showing that all the films are c-oriented. (b) An XRD pattern recorded by tilting the sample at $\psi = 54.7^\circ$, revealing the presence of $(\frac{1}{2} \frac{1}{2} \frac{1}{2})$ and $(\frac{3}{2} \frac{3}{2} \frac{3}{2})$ superstructure reflections.

as given by Brinkman *et al.* (Ref. 20). The order parameter $S \sim 70\%$ is estimated for the PST films. The out-of-plane epitaxial relationship between the films, buffer layers and Si substrate was found to be $(100) \text{PST} // (100)_{\text{pc}} \text{LNO} // (100) \text{CeO}_2 // (100) \text{YSZ} // (100) \text{Si}$ (cubic indexing is used for all; pc—pseudocubic). The in-plane XRD measurements for PST (220), LNO (220), YSZ (220), and Si (220) were done by means of ϕ scans as shown in Fig. 2(a). These in-plane measurements showed that all the films have a four-fold rotational symmetry which confirms the epitaxial growth of all the layers on each other. Both YSZ and CeO_2 films show the same rotational angle as of Si for the (220) reflection, confirming epitaxial cube-on-cube growth. The $(220)_{\text{pc}}$ reflections of LNO and the (220) reflections of PST are shifted by an azimuthal angle of 45° with respect to buffer layer and substrate as shown in schematic in Fig. 2(b). The in-plane epitaxial relationship between the films, buffer layers, and substrate was found to be $[011] \text{PST} // [011]_{\text{pc}} \text{LNO} // [010] \text{CeO}_2 // [010] \text{YSZ} // [010] \text{Si}$. This in-plane rotation of LNO is due to a better lattice match between CeO_2 and LNO: CeO_2 and LNO have (pseudocubic) bulk lattice parameters of 0.541 nm and 0.386 nm, respectively, which allows an almost ideal crystallographic adjustment for LNO to grow diagonally on CeO_2 . It also influences the growth of the PST film with a 45° degree rotation with respect to buffer layers and Si substrate. The full width at half maximum (FWHM) values along (220) reflections for Si, YSZ, CeO_2 , LNO, and PST are $\sim 0.17, 1.44, 0.18, 1.64,$ and 1.35 , respectively, indicating the good crystallinity and good epitaxial growth of PST, LNO, and buffers layers on the Si substrate. In order to analyze the epitaxial relationship between the PST film and the substrate, pole figure measurements were performed, which confirm the single-crystalline nature of the prepared PST films (not shown here). In order to analyze the status of strain present in PST thin films, reciprocal space mapping (RSM) measurements were performed for (440) reflections for Si, YSZ, CeO_2 , and (204) reflections for LNO, PST as shown in Figs. 3(a) and 3(b). The lattice parameter of CeO_2 is close to that of Si, therefore, the reciprocal lattice point of CeO_2 overlaps with that of Si. The in-plane and out-of-plane

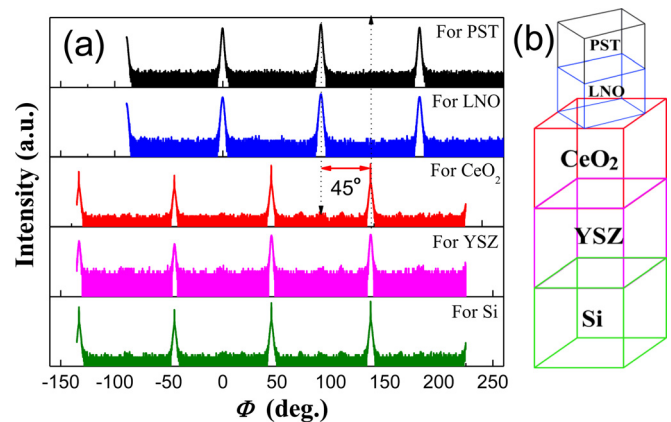


FIG. 2. (a) ϕ -scan using the (220) reflections of PST, LNO, CeO_2 , YSZ thin films, and of the Si substrate. (LNO is pseudocubically indexed.) (b) A schematic demonstrating a 45° in-plane tilt for LNO and PST films with respect to the Si substrate and buffer layers.

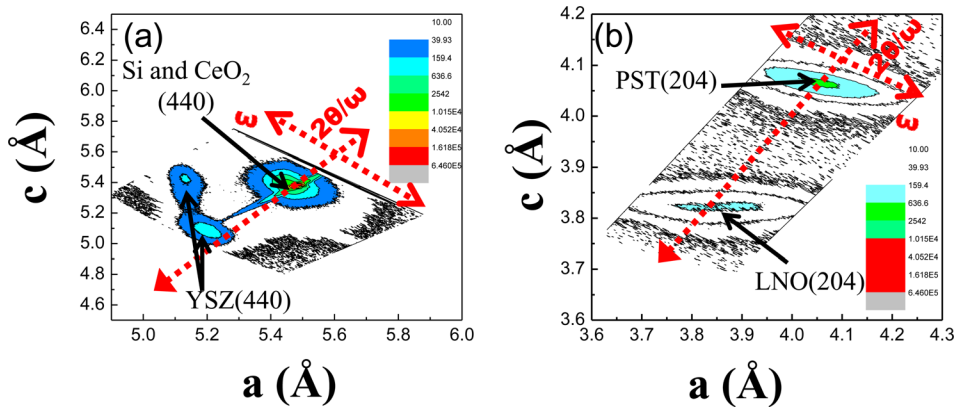


FIG. 3. The reciprocal space maps of the (a) (440) reflections from CeO₂/YSZ/Si (001) epitaxial films and (b) (204) reflections from PST/LNO (001) epitaxial films. The scan directions $2\theta/\omega$ and ω of the two axes are also illustrated.

lattice parameter of Si and CeO₂ have been found to be 5.43 Å (± 0.01). This shows that the CeO₂ layer is fully relaxed on the Si substrate. In case of YSZ, two interconnected reciprocal space patterns were observed. As it is shown in Fig. 3(a), a few layers of YSZ are having the same in-plane lattice parameter as that of Si. The in-plane and out-of-plane lattice parameter values of these few layers of YSZ are 5.43 Å (± 0.01) and 5.10 Å (± 0.01), respectively. This indicates that only few initial YSZ layers were tensile stressed. With increase in thickness of the YSZ layer, the films start to relax and exhibit another reciprocal pattern connected with the stressed layers pattern. The in-plane and out-of-plane lattice parameter for all the buffer layers, electrode, and PST film are tabulated in Table I. The difference between in-plane and out-of-plane lattice parameter values for the LNO film confirms that the films are tensile stressed. The in-plane and out-of-plane parameters for the top PST layer show that the PST film is relatively relaxed on the LNO electrode, although there is still a slight difference between in-plane and out-of-plane lattice parameters.

TEM images [Fig. 4(a)] and selected area electron diffraction (SAED) patterns [inset of Figs. 4(a) and 4(b)] indicate epitaxial growth of the 220 nm thick PST film on the 80 nm thick LNO bottom electrode layer. The thickness of the buffer layers of YSZ and CeO₂ was found to be 55 nm and 115 nm, respectively. The SAED pattern confirms the epitaxial growth of all the layers on the Si wafer with the 45° in-plane rotation, in agreement with the XRD investigations. (In Fig. 4, the LNO reflections are indexed hexagonally.)

Macroscopic and local ferroelectric properties were investigated at room temperature (R.T.). The P - V hysteresis and I - V switching currents measured at 1 kHz [Fig. 5(a)] reveal ferroelectric switching characteristics. The spontaneous polarization P_s , remnant polarization P_r , and coercive

voltage V_c under the application of 5 V are about 14 $\mu\text{C}/\text{cm}^2$, 4 $\mu\text{C}/\text{cm}^2$, and 1.1 V, respectively, which is comparable to the values reported for the PST films on STO substrates.¹⁹ The piezoelectric response of the PST film as a function of applied ac voltage was locally investigated by PFM as shown in Fig. 5(b). The obtained data were linearly fitted to approximate the effective piezoelectric coefficient from the slope of the curve. However, instead of getting one single slope in the fitted data, two slopes were observed, possibly indicating a field driven phase transition. The piezoelectric coefficient at voltages up to 0.6 V was found to be 9.2 pm/V. On applying a higher ac voltage, a sudden increase of the piezoelectric response was observed, the latter amounting to 29.3 pm/V.

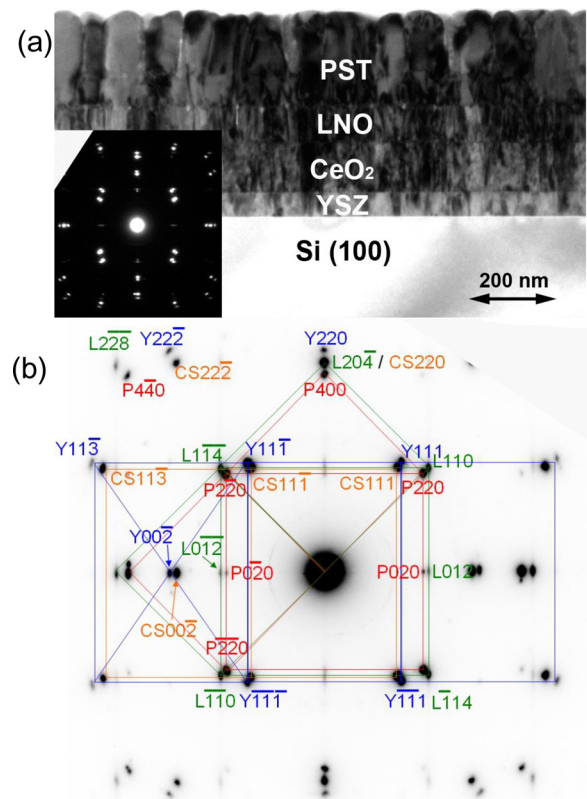


FIG. 4. (a) Cross-section TEM image of a grown heterostructure. Inset: SAED pattern confirming the epitaxial growth of all the layers. (b) Indexed SAED pattern from the inset of (a), however, rotated by 90° for convenient indexing. LNO is indexed hexagonally here. The substrate orientation had been assumed to be Si(010). (P–PST; L–LNO; Y–YSZ; CS–CeO₂ and Si; CeO₂ and Si are not discernible from each other.)

TABLE I. Tabulated values of in-plane and out-of-plane lattice parameters for the different layers including the Si substrate.

Material	In-plane parameter (Å)	Out-of-plane parameter (Å)
Si	5.43	5.43
YSZ	5.14	5.14
CeO ₂	5.43	5.43
LNO	3.85	3.83
PST	4.06	4.05

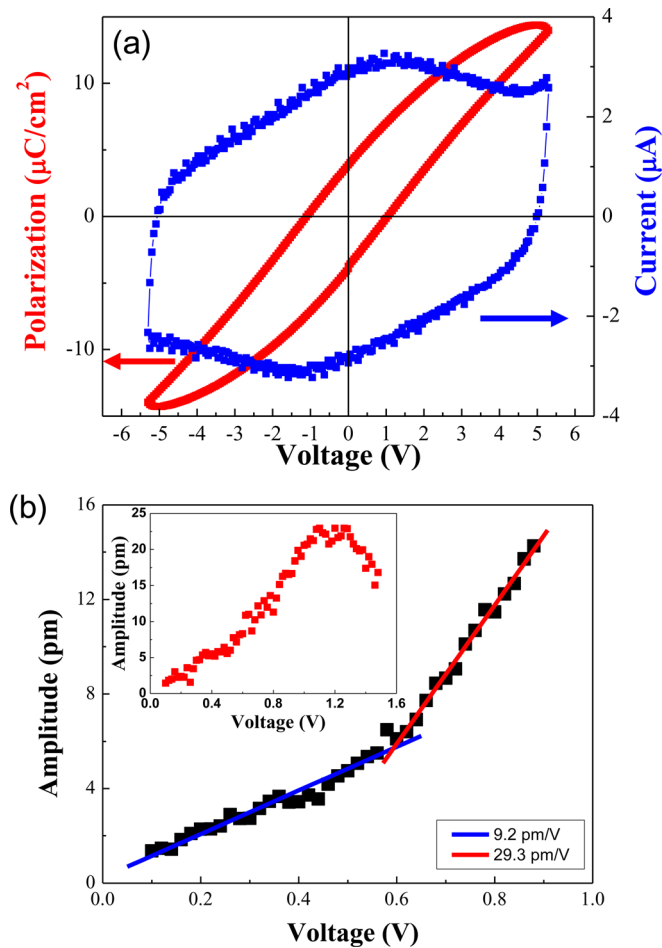


FIG. 5. (a) Macroscopic polarization-voltage and switching current-voltage hysteresis curves of a PST film measured at 1 kHz. (b) Piezoresponse of the PST film as a function of the applied ac voltage. Inset: Demonstration of the coercive voltage by piezoresponse at higher voltage.

This rapid increase may have its origin in an applied-ac-voltage-induced phase transition or percolation of polar nano regions similar as observed in other relaxor based ferroelectrics.^{21–23} The coercive voltage was found to be 1.1 V [inset of Fig. 3(b)], which excludes an effect of the coercive voltage on the sudden increase of the piezoresponse at

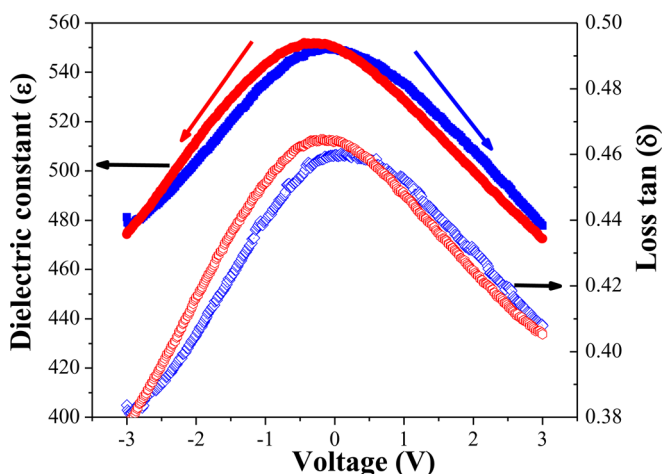


FIG. 6. ϵ -V and $\tan \delta$ -V curves recorded at 100 kHz.

0.6 V. Details of the used experimental conditions during piezoelectric measurements by PFM are reported elsewhere.²⁴ The field dependence of dielectric constant and loss tangent, i.e., ϵ -V and $\tan \delta$ -V curves, were measured at 100 kHz frequency at R.T. [Fig. 6] revealing a butterfly shape and thus supporting the ferroelectric measurements. At a frequency of 1 kHz, the value of the dielectric constant and loss tangent were around 1000 and 0.4, respectively. The measured dielectric constant on buffered Si is higher than previously reported on STO substrate.¹⁴

IV. CONCLUSIONS

In summary, microstructure and ferroelectric properties of epitaxial PST thin films grown on LNO electrodes on YSZ- and CeO₂-buffered Si (100) substrates were investigated. The degree of cation ordering calculated from XRD was around $\sim 70\%$. The results reveal that the films are ferroelectric with a remnant polarization of $4 \mu\text{C}/\text{cm}^2$ at room temperature, which is further confirmed by measuring the C-V and I-V curves. The dielectric constant at 1 kHz was found to be 1000 at room temperature. The sudden increase in the piezoelectric response at 0.6 V suggests the possibility of either a field-driven phase transition or the percolation of polar nano regions in the PST films. Detailed investigations of the piezoelectric non-linearity are under way. Furthermore, this paper shows that the use of epitaxial PST in Si-based technologies is principally possible.

ACKNOWLEDGMENTS

The authors would like to thank Ms. Herrman for TEM sample preparation, and Mr. N. Schammelt for PLD system maintenance. This work was funded by DFG via SFB 762 and Alexander von Humboldt Foundation (Y.K.).

¹M. Kondo, K. Maruyama, and K. Kurihara, *FUJITSU Sci. Tech. J.* **38**, 46 (2002).

²L. E. Cross, *Ferroelectrics* **76**, 241 (1987).

³J. F. Scott, *Ferroelectrics* **183**, 51 (1996).

⁴J. F. Scott, *Science* **315**, 954 (2007).

⁵S. E. Park and T. R. Shroud, *Mater. Res. Innovations* **1**, 20 (1997).

⁶B. I. Birajdar, A. Chopra, M. Alexe, and D. Hesse, *Acta Mater.* **59**, 4030 (2011).

⁷T. M. Correia, S. Kar-Narayan, J. S. Young, J. F. Scott, N. D. Mathur, R. W. Whatmore, and Q. Zhang, *J. Phys. D: Appl. Phys.* **44**, 165407 (2011).

⁸R. W. Whatmore, *Ferroelectrics* **118**, 241 (1991).

⁹N. M. Shorrocks, R. W. Whatmore, and P. C. Osbond, *Ferroelectrics* **106**, 387 (1990).

¹⁰V. Fuflyigin, E. Salley, P. Vakhutinsky, A. Osinsky, J. Zhao, I. Gergis, and K. Whiteaker, *Appl. Phys. Lett.* **78**, 365 (2001).

¹¹C. A. Randall, D. J. Barber, R. W. Whatmore, and P. J. Groves, *J. Mater. Sci.* **21**, 4456 (1986).

¹²L. Corraera and S. Nicoletti, *Mater. Sci. Eng. B* **32**, 33 (1995).

¹³D. K. Fork, D. B. Fenner, G. A. N. Connell, J. M. Phillips, and T. H. Geballe, *Appl. Phys. Lett.* **57**, 1137 (1990).

¹⁴S. J. Wang, C. K. Ong, L. P. You, and S. Y. Xu, *Semicond. Sci. Technol.* **15**, 836 (2000).

¹⁵A. Pignolet, C. Schäfer, K. M. Satyalakshmi, C. Harnagea, D. Hesse, and U. Gösele, *Appl. Phys. A* **70**, 283 (2000).

¹⁶T. W. Chiu, N. Wakiya, K. Shinozaki, and N. Mizutani, *Thin Solid Films* **426**, 62 (2003).

¹⁷M. Dekkers, M. D. Nguyen, R. Steenwelle, P. M. te Riele, D. H. A. Blank, and G. Rijnders, *Appl. Phys. Lett.* **95**, 012902 (2009).

- ¹⁸M. Scigaj, N. Dix, I. Fina, R. Bachelet, B. Warot-Fonrose, J. Fontcuberta, and F. Sánchez, *Appl. Phys. Lett.* **102**, 112905 (2013).
- ¹⁹A. Chopra, B. I. Birajdar, Y. Kim, I. Vrejoiu, M. Alexe, and D. Hesse, *Appl. Phys. Lett.* **95**, 022907 (2009).
- ²⁰K. Brinkman, Y. Wang, D. Su, A. Tagantsev, P. Murali, and N. Setter, *J. Appl. Phys.* **102**, 044110 (2007).
- ²¹F. Li, S. Zhang, Z. Xu, X. Wei, J. Luo, and T. R. ShROUT, *J. Am. Ceram. Soc.* **93**, 2731 (2010).
- ²²M. Davis, D. Damjanovic, and N. Setter, *Phys. Rev. B* **73**, 014115 (2006).
- ²³C. S. Tu, R. R. Chien, C. M. Hung, V. H. Schmidt, F. T. Wang, and C. T. Tseng, *Phys. Rev. B* **75**, 212101 (2007).
- ²⁴Y. Kim, M. Alexe, and E. K. H. Salje, *Appl. Phys. Lett.* **96**, 032904 (2010).